Mathematical Modeling of Rice Cooking and Dissolution in Beer Production

Malcolm J. Davey
Dept. of Mathematics and Statistics, University of Melbourne, Victoria 3010, Australia

Kerry A. Landman
Dept. of Mathematics and Statistics, University of Melbourne, Victoria 3010, Australia

Mark J. McGuinness
School of Mathematical and Computing Sciences, Victoria University of Wellington, Wellington, New Zealand

Hong N. Jin
BrewTech, Carlton & United Breweries Limited, Foster's Brewing Group, Abbotsford, Victoria 3067, Australia

When beer is brewed in Asia, rice is traditionally used as an adjunct to provide additional sugars for the fermentation process. Under sufficiently high temperatures, the grain, which is primarily composed of starch, takes up water. The starch undergoes a gelatinization reaction when the moisture content is sufficiently high. Stirring and enzyme activity facilitate the removal of the outer gelatinized rice layers, and this starch dissolves into solution. The starch molecules are subsequently broken down by enzymes. The water uptake, gelatinization, and dissolution processes are modeled using a modified diffusion approach. The mass of starch molecules dissolved in solution as the cooking proceeds is determined. The dissolution process increases the speed of gelatinization, and the gelatinization front speed and the thickness of the gel layer are constant with time. The modeling takes into account different temperature regimes and a distribution of rice size. Such models help understand and optimize the total dissolved solids from this cooking process.

Introduction

During the beer-making process, adjuncts are generally used to supplement malt starch. Rice is traditionally used in Asia as an adjunct to provide additional sugars, because it is less expensive and readily available compared to cane sugar.

Rice is milled to produce small particles known as grist. The grist is placed into a rice cooker with large quantities of hot water, and the mixture is kept well-stirred. The jacket of the cooker is heated so that the temperature of the mixture rises from around 60°C to 100°C and is held at this temperature for a certain period of time. During this process, the grist, primarily composed of starch, takes up water and swells. The starch undergoes what is called a gelatinization reaction. The shearing effects of stirring remove the gelatinized outer layers and these long-chained starch molecules dissolve into solution, where they are broken up into smaller-chained molecules by enzymes. Enzyme action may also enhance the breakdown and removal of the surface starch molecules. The dissolved starch product is added to another vessel, called the mash tun, to supplement the total amount of sugars obtained from the cooking of malt grist in the presence of malt enzymes.

In this article, we present and solve a mathematical model which estimates the mass of starch molecules dissolved as the cooking proceeds. The modeling is intended to improve understanding of the rice cooking process so the amount of dissolved starch solids can be optimized, and to serve as motivation for further experimental studies. Combining mathematical models and process know-how, the yield of total dissolved solids (that is, yield extract) could be optimized by appropriate choices of the temperature regime, water-to-grist ratio, rice variety, and the size distribution of grist.

Correspondence concerning this article should be addressed to K. A. Landman.

Within an individual rice particle, various processes occur during cooking. The heating, water uptake, and swelling of the rice particle all involve diffusive processes. When water is present at sufficiently high temperatures, the starch undergoes a gelatinization reaction. After gelatinization, the cooked starch molecules are free to dissolve into the liquid medium. Determining the mass of the dissolved starch is our major task. No attempt is made to model the liquefaction process, whereby the dissolved starch undergoes molecular weight reduction by enzymes.

We first focus on understanding and modeling the processes of cooking and dissolution in a single rice particle. This work is then generalized to account for a distribution of grist sizes. A limited sensitivity analysis on temperature regimes and particle-size distribution is also undertaken.

Background to the Modeling

In this section we describe some characteristics of rice (using Juliano (1985) as a major reference), experimental studies of the processes in rice cooking, and polymer dissolution. The assumptions used in our modeling are presented.

A rice grain is primarily composed of starch, with small amounts of proteins, lipids and water. The endosperm is the largest component of the rice grain and the richest in starch. This endosperm is surrounded by many thin bran layers. To produce grist for brewing, the rice is milled to remove these bran layers and break up the endosperm into smaller pieces, around 0.1 to 1.5 mm in size. Depending on the level of milling, about 90% of the dry mass of milled rice is made up of starch. The rice particles are assumed to be spherical in shape.

The starch is enclosed in granules, which are embedded in a protein matrix. The granules are usually 3–9 μm in diameter. There are two types of starch polymers: amylose and amylopectin. Amylose consists mainly of a linear chain, whereas amylopectin has many branching polymer chains and has a more "tree-like" structure. Depending on rice variety, some starch granules are almost entirely composed of amylopectin, whereas others can be quite high in amylose. The organizational structure of these two starch molecules within a granule is complex. Differences between the two types of starch polymers will be ignored here.

Cooking is a common word for describing the starch gelatinization reaction. This occurs in the presence of sufficient water when the temperature is high enough. Studies of the heating, water uptake, and gelatinization processes are now discussed together with their implications for mathematical modeling.

Experimental work on the hydration of grains (Fortes et al., 1981; Kustermann et al., 1981) and recent modeling work (McGowan and McGuinness, 1996) concentrating on a single cereal grain have demonstrated that the conductive heating process proceeds far more rapidly than the hydrating process. Therefore, heat conduction within the grist is ignored and the internal temperature of every rice particle can be taken to be the bulk temperature.

Water motion within a rice particle is driven by a chemical potential gradient which can be written in terms of water activity. This framework gives rise to a Fickian diffusion model for the water uptake. As the water is absorbed by the rice particle, the starch will swell to accommodate the additional water.

Many rice studies have concentrated on the soaking of rice grains at fixed temperatures (Suzuki et al., 1977; Takeuchi, 1997a; Zhang et al., 1975) or on the parboiling process (Bakshi and Sing, 1982; Kar et al., 1999). For temperatures below 50°C, the grains absorb a limited amount of water up to approximately 30% moisture content (wet basis). The resulting grains are not cooked. Cooking occurs at temperatures above 70°C, and takes 20 min or more, depending on the initial moisture content. The moisture content for fully cooked rice grains can rise above 65% moisture content (wet basis).

Recently NMR techniques have been used to analyze moisture profiles for starchy materials. During the boiling of wheat grains, Stapley (1995) found fairly sharp moisture fronts which moved approximately linearly with time. This suggests possible similarities with non-Fickian diffusion of liquid solvents into polymers (Thomas and Windle, 1982). Such behavior may be distinguished by a sharp penetrant front that moves at a constant velocity and the resulting solvent uptake rate is constant with time. However, for wheat grains, the front is not a severe discontinuity in concentration since moisture also diffuses ahead of the front. This suggests that the diffusion process may be anomalous, meaning that it lies between purely Fickian and purely non-Fickian diffusion. However, the linear fronts seen in wheat grains can also be explained with a purely Fickian diffusion model for moisture uptake, if the finite resistance of the outer pericarp of the wheat is taken into account (Landman and Please, 1999). Since individual rice particles in grist have no outer pericarp and consist of pure endosperm only, this model is not appropriate here. Some NMR work has recently been undertaken for rice grains (Takeuchi et al., 1997a,b) but the conclusions are not as clear as for Stapley's wheat experiments.

Using NMR and other techniques, the moisture diffusivity has been carefully measured for wheat (Stapley, 1995), for rice starch/water mixtures (Gomi et al., 1998), and for corn kernel (Syarief et al., 1986). The diffusivity is found to be a strongly increasing function of moisture content, which can be fitted to either a power law or an exponential form. A Fickian model for water uptake gives rise to nonlinear diffusion equations inside a swelling sphere.

As water is taken up by a rice particle, the starch granules may undergo a gelatinization reaction, the term generally used to describe the swelling and hydration of the granular starch (Whistler et al., 1984). With adequate water, gelatinization occurs if the temperature is high enough, and the swelling is irreversible. There is a minimum temperature $T_{g\min}$ at which gelatinization begins to occur, and usually a temperature range of about 10°C over which gelatinization occurs in a ramping temperature environment. Below $T_{g\min}$, starch granules swell slightly, but the swelling is reversible (van Beynum, 1985). In its narrowest sense gelatinization is the thermal disordering of crystalline structure in native starch granules (Tester and Morrison, 1990). A thorough literature review on gelatinization is to be found in Stapley (1985).

The gelatinization temperature and the amount and speed of swelling are influenced by the ratio of amylopectin to amylose, the amount of other material such as lipids and proteins, as well as the initial water content and the size of the starch granules. The minimum gelatinization temperature for

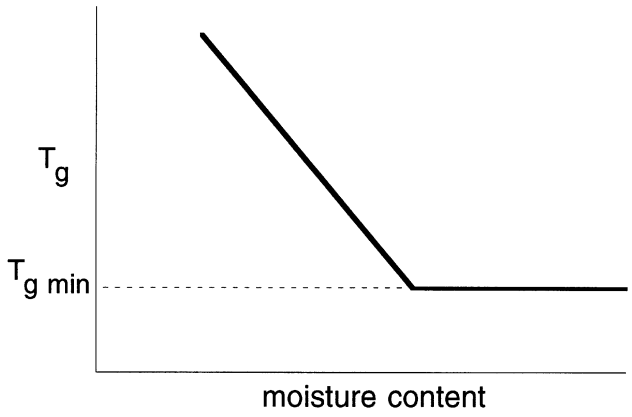

Figure 1. Gelatinization temperature vs. moisture content.

rice is usually around 68–75°C, although the exact temperature varies between different types of grain, and between granules of the same grain (Juliano, 1985; Lund and Wirakartakusumah, 1984). The temperature of gelatinization increases with decreasing availability of water (Biliaderis et al., 1986; Juliano, 1985). The experimentally derived relationship between local moisture content and gelatinization temperature is shown in Figure 1.

Suzuki and coworkers (Suzuki et al., 1976, 1977) measure the proportion of the soft rice grain at different cooking times, for a large range of cooking temperatures. From this data, a cooking rate constant as a function of temperature is estimated and thought to change at around 110°C. They attribute this change to whether the gelatinization reaction rate or the water diffusion rate is the rate-determining mechanism at the given temperature. Their cooking model has a shrinking un-cooked core, and conservation of mass principles are applied to set up simple rate equations.

The main goal of the cooking process under investigation is to free starch molecules from the grist, allowing enzymes to break these large molecules into small molecular weight sugars. After the starch granules have been gelatinized, the starch molecules must escape from the rice particle and dissolve into the bulk solution.

The process of dissolution is of little concern when using flours instead of whole rice grains or grist, because the flour particle sizes are much smaller and, hence (provided there is no agglomeration taking place), dissolution occurs very rapidly. For this reason, many texts on brewing ignore the dissolution process and consider only gelatinization followed directly by liquefaction and saccharification (Kunze, 1996).

For low molecular weight nonpolymeric species, the dissolution rate is predominantly governed by the mass-transfer resistance (Devotta et al., 1994a; Rande and Mashelkar, 1995). The overall rate of mass transfer is indirectly a function of the particle size through being a function of exposed surface area. If a particle is cut in half, then it has more exposed surface and so dissolution can occur from this new surface.

For high molecular weight polymers, the dissolution process is much more complicated, because the long chains must first disentangle themselves before they are able to dissolve in solution.

A reptation model for the behavior of entangled polymers has been developed (de Gennes, 1979) and applied to the dissolution of polymers (Herman and Edwards, 1998; Papanu et al., 1989). One of the key elements of this model is that a polymer chain requires a certain amount of time, called the reptation time, to become disentangled from a polymer network. Reptation is a complicated process, which depends on molecular weight among other factors (Tsiartas et al., 1997). After solvent uptake by the polymer network, dissolution will begin only after there has been sufficient time for reptation to be completed. As a consequence, there is a critical particle size, below which the dissolution time is no longer dependent on the size of the particle, but depends on reptation time (Devotta et al., 1994a; Ranade and Mashelkar, 1995). Devotta et al. (1994a) obtained the first experimental results that showed the existence of a critical particle size. This is in marked contrast to the dissolution of nonpolymeric low molecular weight compounds, where a smaller particle size always leads to a faster dissolution rate.

There are additional factors influencing the rate of dissolution of starch. Amylose and amylopectin, the two types of starch polymers, behave differently after gelatinization has occurred, because of their different structure and size.

One of the implications of this theory is that if the mass-transfer rate is higher than the reptation rate, then the dissolution process will be limited by the rate of reptation. On the other hand, if mass transfer is slower and, therefore, rate limiting, then reptation will not be as important (Papanu et al., 1989).

There is evidence during the industrial rice cooking process that the rate of dissolution depends on stirring rate. One explanation of this effect is that once the starch is gelatinized and reptation has occurred, the starch polymers are sheared away from the grist surface by the stirring, and, consequently, the cooked starch at the boundary of the rice particle will more readily dissolve into the liquid solution. The enzymes in the liquid reduce the molecular weight of the starch. If the enzymes can diffuse into the gel layer, or act on the surface elements, then the molecular weight of the components may be reduced directly there and, hence, increase the mass-transfer rate and promote more rapid dissolution. We do not specifically attempt to model these effects, but we do investigate the effects of various magnitudes of dissolution rates in our model, and we also allow dissolution rates to vary in a specific way in a later section where we examine conditions for complete dissolution of the rice starch.

Analysis for a Single Grain

In this section a mathematical model for water uptake, gelatinization, and dissolution is developed for a single rice particle. Derivation of the water uptake model where the particle swells due to absorption of water is readily available in the literature (Stapley et al., 1998; Landman and Please, 1999; McGuinness et al., 2000).

Let ϕ be the volume fraction occupied by water, while $1-\phi$ is the volume fraction of solid, assumed here to be all starch. Assuming that the fluid and solid velocities are in a radial direction, arguments involving mass conservation and Darcy's law applied to flow in a moving solid yield a nonlinear diffusion equation describing the water uptake in the starchy

porous media. Replacing an arbitrarily-shaped piece of rice with an equivalent spherical grain of effective radius R, the water volume fraction $\phi(r,t)$ satisfies

$$\frac{\partial \phi}{\partial t} = \frac{1}{r^2}\frac{\partial}{\partial r}\left[r^2 D(\phi)\frac{\partial \phi}{\partial r}\right] \tag{1}$$

where $D(\phi)$ represents the moisture diffusivity.

Since the inhibiting outer pericarp has been milled from the rice, the concentration at the boundary is assumed to be a constant value corresponding to equilibrium or saturation, and it is written as

$$\phi(R(t),t) = \phi_1 \tag{2}$$

Experimental work indicates that ϕ_1 may vary with temperature (Takeuchi et al., 1997b) for temperatures above 50°C. For fixed temperature, clearly ϕ_1 is a constant.

As water is absorbed, the sphere will swell giving an evolving surface radius $R = R(t)$. To generate an equation for the rate of change of $R(t)$ with time, the total mass inside the swelling sphere is determined by integrating Eq. 1 over the solid spherical volume as

$$\int_0^{R(t)} \frac{\partial \phi}{\partial t} r^2 dr = \int_0^{R(t)} -\frac{\partial (1-\phi)}{\partial t} r^2 dr = \int_0^{R(t)} \frac{\partial}{\partial r}\left[r^2 D(\phi)\frac{\partial \phi}{\partial r}\right] dr \tag{3}$$

Using Leibniz's rule to interchange the time derivative and spatial integration, and noting that $\frac{\partial \phi}{\partial r}(0,t) = 0$, the outer boundary $R(t)$ is then found to obey the equation

$$R^2 \frac{dR}{dt} = \left(\frac{D(\phi_1)}{1-\phi_1}\right) R^2 \frac{\partial \phi}{\partial r}[R(t),t] + \frac{1}{(1-\phi_1)}\frac{d}{dt}\left[\int_0^{R(t)} (1-\phi) r^2 dr\right] \tag{4}$$

The lefthand side is proportional to the rate of change of the spherical volume. The first term on the righthand side represents the flux of water through the grain surface contributing to the increase in the volume of the swelling sphere. The second term is proportional to the time rate of change of the total volume of solids in the rice particle. This term accounts for any possible solids loss and will be negative when there is dissolution of solids. Hence, dR/dt is given by the difference between swelling rate and dissolution rate.

We assume that the water is initially uniformly distributed inside the rice particle, so that

$$\phi(r,0) = \phi_0 \tag{5}$$

The moisture diffusivity is a strongly increasing function of moisture content and the diffusivity is much larger in gelatinized starch than ungelatinized starch. Then, there is a steep moisture front between the dry/ungelatinized/uncooked and wet/gelatinized/cooked regions of a particle, and, furthermore, gelatinization occurs at this front. We denote the position of this front as $s(t)$. For a given temperature, gelatinization occurs at a certain moisture volume fraction denoted as ϕ_g (as illustrated in Figure 1); hence, we write

$$\phi(s(t),t) = \phi_g \tag{6}$$

Furthermore, we assume that the diffusivity is discontinuous at $s(t)$ (Stapley et al., 1998). Since the diffusivity is very much smaller ahead of the front than behind the front, for simplicity, we assume that $D(\phi)$ is zero for $\phi < \phi_g$. This assumption will not affect the front speed significantly, because the limiting process is the transport at the front. Hence, we assume that no moisture diffuses ahead of the gelatinization front giving $\phi(r,t) = \phi_0$ for $0 \le r < s(t)$. The gelatinization front is approximated by a water volume fraction discontinuity or shock at $\phi(s(t),t) = \phi_g$, namely

$$\phi(s^+,t) = \phi_g, \quad \phi(s^-,t) = \phi_0 \tag{7}$$

An equation for the motion of this discontinuity can be obtained by performing a mass balance across the discontinuity. Multiplying Eq. 1 by r^2, integrating across the front from $r = s^-$ to $r = s^+$ gives

$$\frac{d}{dt}\int_{s^-}^{s^+} \phi r^2 dr - (\phi_g - \phi_0) s^2 \frac{ds}{dt} = \left[s^2 D(\phi)\frac{\partial \phi}{\partial r}(s(t),t)\right]_{s^-}^{s^+} \tag{8}$$

Using $D(\phi_0) = 0$ and letting s^+ and s^- tend towards the gelatinization front $s(t)$ allows Eq. 8 to be rearranged as

$$\frac{ds}{dt} = -\frac{D(\phi_g)}{\phi_g - \phi_0}\frac{\partial \phi}{\partial r}(s(t),t) \tag{9}$$

This equation describes the evolution of the gelatinization front, which marks the boundary between cooked and uncooked portions of the rice particle. Note that it depends strongly on the change in moisture across the front, and on the profile in the wet/cooked region, consistent with our assumption that moisture diffusion in the uncooked region has a negligible effect.

Note that gelatinization occurs over a range of temperatures and moisture levels, while it is localized to the steep front in our model. Furthermore, in taking the front to move in a manner dictated only by the moisture balance and moisture diffusion, we are assuming that any gelatinization kinetics are rapid enough that they are not rate-limiting at the front.

The spatial variable, outer radius, gelatinization front radius, volume fraction, time and the diffusivity function are scaled according to

$$\bar{r} = \frac{r}{l},\ \bar{R} = \frac{R}{l},\ \bar{s} = \frac{s}{l},\ \theta = \frac{\phi - \phi_0}{\phi_1 - \phi_0},\ \bar{t} = \frac{D(\phi_1)}{l^2}t,\ \mathfrak{D}(\theta) = \frac{D(\phi)}{D(\phi_1)} \tag{10}$$

where l is the initial radius of the sphere. Note that here the equilibrium moisture volume fraction can be a function of the temperature T. Clearly, for a cooking process held at a constant temperature, ϕ_1 is fixed. However, if the temperature is allowed to vary over the course of the cooking operation, the scaling used here must be modified to take into account any temperature dependence of the diffusivity (see Appendix B). In the treatment here it will be assumed that the temperature is held constant throughout the cooking process. Since we are modeling the water uptake and gelatinization, that is, the cooking of rice and not just the soaking of rice, the chosen temperature is assumed to be above the minimum gelatinization temperature indicated in Figure 1.

For convenience, the overbar notation will be dropped when the context is clear. In dimensionless terms, Eq. 1 becomes

$$\frac{\partial \theta}{\partial t} = \frac{1}{r^2}\frac{\partial}{\partial r}\left[r^2 \mathfrak{D}(\theta)\frac{\partial \theta}{\partial r}\right] \tag{11}$$

This nonlinear diffusion equation has the following boundary and initial conditions

$$\theta(r,0) = 0, \quad \theta(R(t),t) = 1, \quad \theta(s(t),t) = \theta_g, \quad R(0) = 1 \qquad s(0) = 1 \tag{12}$$

where θ_g is just the scaled gelatinization moisture content

$$\theta_g = \frac{\phi_g - \phi_0}{\phi_1 - \phi_0}$$

Since ϕ_g decreases with increasing temperature and ϕ_1 may increase with increasing temperature, the variable θ_g must decrease with increasing temperature.

In dimensionless terms, Eqs. 4 and 9 describing the evolution of the outer boundary and the gelatinization front become

$$\frac{dR}{dt} = \alpha \frac{\partial \theta}{\partial r}(R(t),t) - \lambda \tag{13}$$

$$\frac{ds}{dt} = -\beta \frac{\partial \theta}{\partial r}(s(t),t) \tag{14}$$

where we have introduced parameters α and β defined by

$$\alpha = \frac{\phi_1 - \phi_0}{1 - \phi_1}, \quad \beta = \frac{D(\phi_g)}{D(\phi_1)}\left(\frac{\phi_1 - \phi_0}{\phi_g - \phi_0}\right) = \frac{\mathfrak{D}(\theta_g)}{\theta_g} \tag{15}$$

For the constant temperature T, the parameters α and β are constants. We have also introduced a term λ which represents the dimensionless solid dissolution rate defined as

$$\lambda(t) = -\frac{1}{(1-\phi_1)R^2}\frac{d}{dt}\left[\int_0^{R(t)}(1-\phi)r^2 dr\right] \tag{16}$$

Pseudo-steady-state approximation

The water uptake, gelatinization, and dissolution processes inside the spherical rice particle are described by the nonlinear diffusion Eq. 11 with two moving boundaries. In order to gain insight into the movement of the gelatinization front into a swelling piece of rice, we chose to explore approximate analytic solutions.

The approach below has been adopted by other authors for similar nonlinear problems (Landman and Please, 1999; Landman et al., 2001; McGowan and McGuinness, 1996; McGuinness et al., 1998, 2000). We consider the case where the moisture content changes substantially and the water diffusivities at the initial and final moisture contents are an order of magnitude different. Under such circumstances, because the diffusivity is such a strong function of the moisture content, water penetrates the grain as a steep front. The outer cooked region is almost at diffusive steady state, so that the moisture profile there is termed pseudo-steady or quasi-steady state, while there is little moisture transfer in the inner core, and the two zones are separated by the gelatinization front $s(t)$. Hence, in the outer region we set $\partial\theta/\partial t \approx 0$.

In spherical coordinates, the diffusion Eq. 11 in pseudo-steady state reduces to

$$\frac{\partial}{\partial r}\left[r^2 \mathfrak{D}(\theta)\frac{\partial \theta}{\partial r}\right] = 0 \tag{17}$$

Integrating this implies that the moisture profile θ satisfies the implicit relation

$$\Gamma(\theta) = \frac{A(t)}{r} + B(t) \tag{18}$$

where

$$\Gamma(\theta) = \int_0^{\theta} \mathfrak{D}(\omega)\, d\omega \tag{19}$$

Note that Γ is the Kirchoff transformation commonly introduced in nonlinear diffusion problems (Kirchoff, 1894). After applying the moisture boundary conditions (Eq. 12), we find that the moisture profile satisfies the following equation

$$\frac{\Gamma(\theta) - \Gamma(\theta_g)}{\Gamma(1) - \Gamma(\theta_g)} = \frac{\dfrac{1}{s(t)} - \dfrac{1}{r}}{\dfrac{1}{s(t)} - \dfrac{1}{R(t)}} \tag{20}$$

This equation implicitly relates θ and r at some time t, given R and s.

Equations determining the time evolution of R and s are obtained by differentiating Eq. 20 with respect to r, and substituting into Eqs. 13 and 14 to give

$$\frac{dR}{dt} = \Omega_1 \frac{1}{R^2\left(\dfrac{1}{s} - \dfrac{1}{R}\right)} - \lambda \tag{21}$$

$$\frac{ds}{dt} = -\Omega_2 \frac{1}{s^2\left(\dfrac{1}{s} - \dfrac{1}{R}\right)} \tag{22}$$

where

$$\Omega_1 \equiv \alpha\left[\Gamma(1) - \Gamma(\theta_g)\right] \tag{23}$$

$$\Omega_2 \equiv \frac{\Gamma(1) - \Gamma(\theta_g)}{\theta_g} \tag{24}$$

At constant temperature T, Ω_1 and Ω_2 are constant. The position $R(t)$ represents the location of the outer boundary and dissolution front. These equations are only valid up to the time that the gelatinization front reaches the center of the rice particle. A similar treatment is used for the dissolution of polymers (Devotta et al., 1994a,b; Papanu et al., 1989).

In the following sections we study the solutions to our model for the case of constant temperature. The case of varying temperature is the subject of Appendix B.

Analytic solutions for constant temperature

No Dissolution. For the case $\lambda = 0$, Eqs. 21–22 can be combined and solved exactly in the case of constant temperature, giving the following expressions

$$R^3 + \frac{\Omega_1}{\Omega_2} s^3 = 1 + \frac{\Omega_1}{\Omega_2} \tag{25}$$

Equation 25 can be rearranged to express s as an explicit function of R

$$s \equiv S(R) = \left[\frac{\Omega_2}{\Omega_1}\left(1 + \frac{\Omega_1}{\Omega_2} - R^3\right)\right]^{1/3} \tag{26}$$

Substituting this into Eq. 21 permits integration to give an implicit expression for R as

$$\left(1 + \frac{\Omega_1}{\Omega_2}\right) - \left(R^2 + \frac{\Omega_1}{\Omega_2} S^2\right) = 2\Omega_1 t \tag{27}$$

It can be shown that $1 - s(t)$ and $R(t) - 1$ are both proportional to $\sqrt{t}$ for small t as is expected for diffusive processes.

We now determine the gelatinization time, that is, the time when the gelatinization front reaches the center of the rice particle. First, the radius of the sphere at this time can be found by setting $s = 0$ in Eq. 25, giving the maximum radius of the swelled rice particle as

$$R_g = \left(1 + \frac{\Omega_1}{\Omega_2}\right)^{1/3} \tag{28}$$

This implies that when gelatinization is complete, the volume expansion factor of a single grain VEF is given by

$$\text{VEF} = 1 + \frac{\Omega_1}{\Omega_2} = 1 + \alpha\theta_g \tag{29}$$

The time required for the rice particle to be fully gelatinized is then determined from Eq. 27 by setting $S = 0$ and $R = R_g$ as

$$t_g = \frac{1}{2\Omega_1}\left[\left(1 + \frac{\Omega_1}{\Omega_2}\right) - \left(1 + \frac{\Omega_1}{\Omega_2}\right)^{2/3}\right] \tag{30}$$

Nonzero Dissolution. For the case $\lambda > 0$, no general analytic solutions are available. However, we can obtain asymptotic solutions for the case that λ is constant and sufficiently large. Then, dissolution occurs rapidly compared to gelatinization, and the dissolution front R is expected to remain close to the gelatinization front s. We observe this to be true in our numerical results in a later section, and this is also consistent with the results presented by Peppas et al. (1994). Therefore, dissolution will be almost complete when $s(t) = 0$, and the system Eqs. 21–22 can be used to give an approximation for the dissolution time.

We set $R = s + \delta_p$, so that δ_p represents the thickness of the region between the gelatinization front and the dissolution front; it is expected to be small. Then, Eqs. 21–22 can be rewritten as

$$\frac{dR}{dt} = \frac{\Omega_1}{\delta_p}\frac{s}{R} - \lambda \tag{31}$$

$$\frac{ds}{dt} = -\frac{\Omega_2}{\delta_p}\frac{R}{s} \tag{32}$$

Since $R(0) - s(0) = \delta_p(0) = 0$, initially and for early times, $dR/dt > 0$ and $ds/dt < 0$. Hence, $d(R - s)/dt > 0$ so that the thickness of the gelatinized shell $R(t) - s(t)$ increases. Provided $\delta_p \ll s$, δ_p reaches the following asymptotic size

$$\delta_p \sim \frac{\Omega_1 + \Omega_2}{\lambda} \tag{33}$$

When s is order one, $\delta_p \ll s$ requires that

$$\lambda \gg \Omega_1 + \Omega_2 \tag{34}$$

When the shell thickness reaches the asymptotic size (Eq. 33), this relation may be used to eliminate λ. Then, the two differential equations are the same, so that $dR/dt \approx ds/dt \approx -\Omega_2/\delta_p$. Hence, in this regime the shell thickness is almost constant with approximate thickness $(\Omega_1 + \Omega_2)/\lambda$. At later times, s accelerates towards zero. For larger values of the parameter λ, the approximations of constant $R - s$ and, hence, constant dR/dt and ds/dt remain valid for a larger proportion of the process. Hence, for a given λ, the approximate thickness of the gelatinized region is given by Eq. 33.

Under this requirement, an estimate of the speed of the dissolution front v_d can be determined using the approximations

$$v_d \approx -\frac{dR}{dt} \approx \frac{\Omega_2}{\delta_p} = \frac{\lambda}{1 + \frac{\Omega_1}{\Omega_2}} \tag{35}$$

In dimensionless terms, since the front travels a unit distance, the dissolution time t_d is well approximated by $1/v_d$

$$t_d = \frac{1}{\lambda}\left(1 + \frac{\Omega_1}{\Omega_2}\right) \tag{36}$$

Numerical solutions for constant temperature

Here, we numerically determine the locations of $s(t)$ and $R(t)$ by solving the system of differential Eqs. 21–22. We first choose an appropriate diffusivity function at fixed temperature with exponential form as

$$D(\phi) = Ae^{c\phi} \tag{37}$$

where A and c are experimentally determined constants. With this choice, the corresponding function $\Gamma(\theta)$ is

$$\Gamma(\theta) = \frac{1}{\nu}(e^{\nu(\theta-1)} - e^{-\nu}) \tag{38}$$

where

$$\nu = c(\phi_1 - \phi_0) \tag{39}$$

Note that R and s will now depend on the values of ν and θ_g.

Diffusivity measurements for ground rice starch/water mixtures are reported by Gomi et al. (1998). These estimates are expected to be larger than those for whole rice grains. The measurements were fitted to a sum of exponential functions over a wide range of the wet basis moisture contents. In terms of the volume fraction ϕ, these can be fitted just as well by the simple exponential form (Eq. 37) as

$$D(\phi) = 1.43\times10^{-7}e^{5.22\phi}\ \text{cm}^2/\text{s at } 25^\circ\text{C}$$

Without further data, we choose $c = 5.22$ here. The value of $D(\phi_1) = Ae^{c\phi_1}$ is needed for the time scaling; this quantity is expected to be substantially smaller than the value calculated from Gomi's numbers. However, the accurate determination of diffusivity and its dependence on moisture content is still needed for whole grain milled rice before the results in this article can be confidently quantified. As discussed earlier, the equilibrium moisture volume fraction ϕ_1 may vary for temperatures above 60°C. Data for this is inconclusive, although it is agreed that in boiling or close to boiling situations, the wet basis moisture content is approximately 0.73 (Juliano, 1985; Ramesh and Srinivasa Rao, 1996). This converts to a moisture volume fraction of approximately 0.8. In general, we might expect ϕ_1 to decrease from this value as temperature decreases.

Table 1a. Parameter Values Used for Calculating Water Uptake and Gelatinization Rates

Constant	Value
Initial mass (wet basis)	14%
Initial rice density	1.43 g/L
ϕ_0	0.2
Equilib. mass (wet basis)	73%
ϕ_1	0.8
c	5.22
ν	3.13
α	3

Table 1b. Parameter Values as a Function of θ_g

θ_g	Ω_1	Ω_2	VEF $= 1+(\Omega_1/\Omega_2)$	t_g
0.2	0.88	1.47	1.6	0.13
0.3	0.85	0.95	1.9	0.22
0.4	0.81	0.68	2.2	0.31
0.5	0.76	0.51	2.5	0.43
0.6	0.68	0.38	2.8	0.59
0.7	0.58	0.28	3.1	0.83
0.8	0.45	0.19	3.4	1.28
0.9	0.26	0.10	3.7	2.54

As noted earlier, as temperature decreases, $\theta_g(T)$ increases. Using the parameter values in Table 1a for our calculations, typical values of Ω_1 and Ω_2 can be obtained, as shown in Table 1b. Note that the parameters Ω_1 and Ω_2 decrease with increasing θ_g, whereas the ratio Ω_1/Ω_2 increases with increasing θ_g.

For the case of no dissolution ($\lambda = 0$), the positions of $R(t)$ and $s(t)$ for different values of θ_g are illustrated in Figures 2 and 3. These figures are qualitatively the same as the results of McGuinness et al. (1998, 2000). If more water absorption is required for gelatinization, the time required will increase, so that t_g increases with increasing θ_g. This in turn gives an increase in the amount of swelling. Note that in the limit as $\theta_g \to 1$, the rice particle comes to equilibrium moisture content (in infinite time) and the VEF $\to 4$ for this choice of parameter values. This is the approximate value obtained experimentally by Ramesh and Srinivasa Rao (1996).

The case of nonzero dissolution is illustrated in Figure 4. For sufficiently large λ, R and s are almost linear with time over their full range, and the thickness of the gelatinized region $R - s$ is approximately constant, as predicted by the analysis above. For smaller values of δ_p, the approximation for the dissolution time is very good; for example, with $\lambda = 50$, the numerical solution gives $R = 0$ at a time equal to 0.051, whereas the approximation (Eq. 36) for the dissolution time gives 0.056. (For these figures, after $s = 0$, the R equation

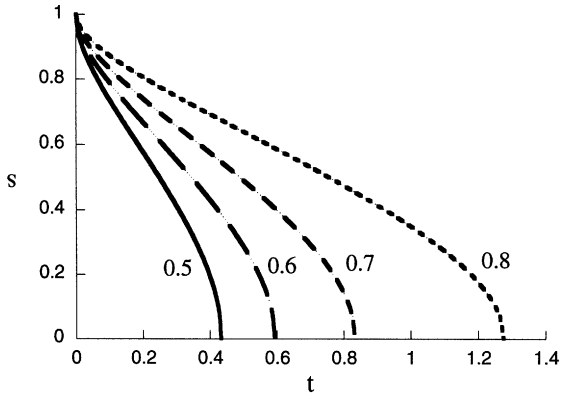

Figure 2. $s(t)$ using parameter values in Table 1a and various values of θ_g as shown.

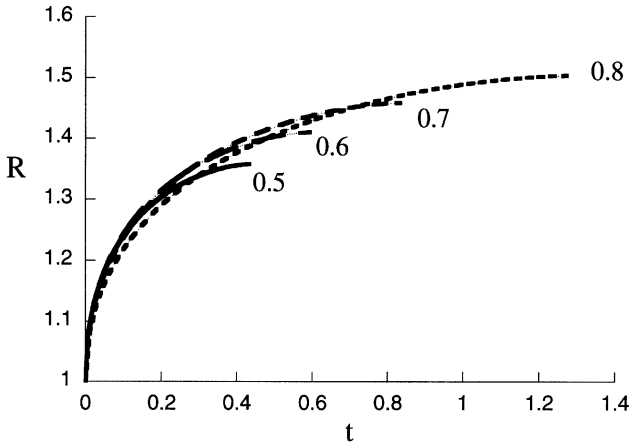

Figure 3. $R(t)$ using parameter values in Table 1a and various values of θ_g as shown.

has been approximated by $dR/dt = -\lambda$.) If Eq. 34 is not satisfied, then $R(t)$ increases for some time since water uptake and, hence, swelling dominates over dissolution. The $s(t)$ has a similar shape to that in the no dissolution limit, as illustrated in Figure 2.

In practice if the choice of parameters satisfies the condition (Eq. 34), we find that the constant thickness approximation dominates over most of the dissolution process. Our results illustrated in Figure 4 are similar to the numerical and experimental results of Peppas et al. (1994). Their figures also show constant front speeds with a gel region of constant thickness. The short time behavior of their numerical results shows swelling of the grain (R increasing) as we have shown in our example with $\lambda = 1$. Their particular disentanglement model for dissolution initially has no dissolution, thus, giving rise to swelling; this is followed by a sudden change in direction of the outer surface when dissolution commences. Their experimental results show a change in direction of the polymer surface which is less sudden than the predictions of their model, which are more like our results. The long time behavior of the graphs here and in Peppas et al. are different be-

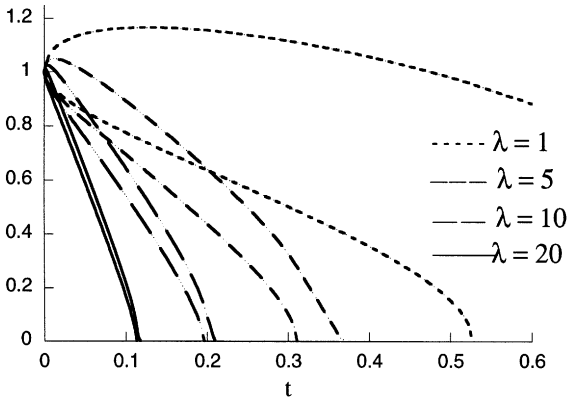

Figure 4. $R(t)$ and $s(t)$ using parameter values in Table 1a, $\theta_g = 0.6$ and various values of λ.

For each pair with a fixed λ, the R curves lie above the s curve. Eq. 34 becomes $\lambda \gg 1.06$.

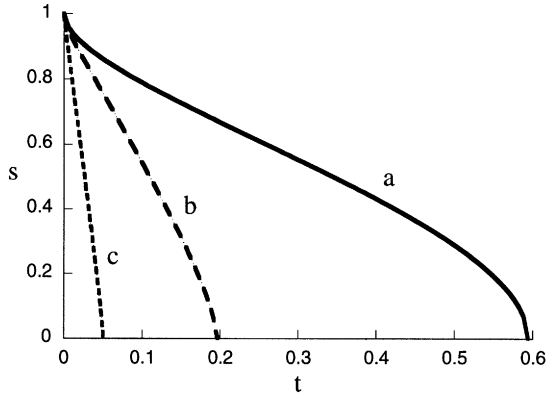

Figure 5. $s(t)$: (a) No-dissolution model, (b) dissolution model with $\lambda = 10$, and (c) dissolution model with $\lambda = 50$.

The parameter values are in Table 1a with $T = 91$°C corresponding to $\theta_g = 0.6$.

cause of the difference in geometry. The polymer dissolution model of Edwards and Cohen (1995) which incorporates non-Fickian diffusion also gives constant front speeds.

The positions of the gelatinization front $s(t)$ obtained in the cases of zero dissolution and nonzero dissolution are compared in Figure 5. In the absence of dissolution, the gelatinization front is initially proportional to $\sqrt{t}$ and it accelerates as it approaches the particle center. When the dissolution rate λ is nonzero, and if the relationship between the dissolution and gelatinization parameters satisfies the requirement in Eq. 34, a faster gelatinization front is observed, one that moves at a constant rate. As the dissolution rate increases, the process becomes increasingly rapid.

Discrete interpretation of dissolution

It is interesting to interpret our continuous model of dissolution alternatively as a discrete model, as detailed in the analysis presented in Appendix A for the case of large dissolution rate. Then, the rice particle interior is taken to consist of concentric spherical shells of starch granules. The entire spherical shell of starch granules at the boundary, once ruptured by gelatinization, is assumed to immediately peel away from the rice particle. Let Δ be a measure of the size of a starch granule, scaled by the initial radius of the sphere, so that $l\Delta$ represents the real physical granule size. We assume that a shell of starch granules is removed from the particle once all the granules in the shell are gelatinized. Hence, the region between R and s is removed and goes into solution. These shells will be removed one at a time, as the gelatinization front progresses into the rice particle.

Both the continuous and discrete models give constant front speeds over most of the process time. By comparing them, an expression for the thickness of a swollen gelatinized layer in the continuous model δ_p can be found in terms of the discrete unswollen peeling thickness Δ as

$$\delta_p = \left(1 + \frac{\Omega_1}{\Omega_2}\right)\frac{\Delta}{2} \tag{40}$$

This relationship is interpreted geometrically in Appendix A.

Furthermore, the relationship

$$\frac{2\Omega_2}{\Delta} = \lambda \tag{41}$$

from Appendix A provides a physical link between the rate λ and the size Δ of a granule of starch.

Total Dissolved Solids

The cooking and dissolution model developed above allows for the estimation of the mass of starch molecules dissolved as the cooking proceeds. Using the realistic approximation that the solids are composed entirely of starch, an expression describing the total volume of solids dissolved will be examined: first for the case when all grains in the grist have the same size, and then for an arbitrary distribution of grist sizes.

Grain of uniform size

In dimensionless terms, the solids volume in a single spherical rice particle at time t is

$$V_s(t) = 4\pi\int_0^{R(t)}(1-\phi)r^2 dr \tag{42}$$

which converts into a dimensioned solids mass of $M_s(t) = l^3\rho_s V_s(t)$. The dimensionless solids volume which has been removed from the particle and, therefore, dissolved is

$$V_d(t) = V_s(0) - V_s(t) = \frac{4\pi(1-\phi_0)}{3} - V_s(t) \tag{43}$$

However, in order to determine the solids volume $V_d(t)$ using Eq. 42, the moisture content $\phi(r,t)$ (or $\theta(r,t)$) must be determined. For full accuracy, this must be calculated numerically with either the full nonlinear diffusion equations or through the pseudo-steady-state approximations (valid for $t \le t_g$).

Alternative calculations of the dissolved solids volume can be obtained by the first differentiating Eq. 43 with respect to t and recalling the definition of the dissolution rate λ from Eq. 16. This manipulation gives

$$\frac{dV_d}{dt} = 4\pi\lambda(1-\phi_1)R^2(t) \tag{44}$$

Equation 44 shows that the rate of increase of total dissolved solids is proportional to R^2. For a constant dissolution rate λ, this means the rate of increase of dissolved solids volume decreases as the surface area of the particles decreases. Therefore, continuing the dissolution process becomes less worthwhile as time progresses. Integrating Eq. 44 gives

$$V_d(t) = V_s(0) - V_s(t) = 4\pi(1-\phi_1)\int_0^t \lambda R^2(\tau)d\tau \tag{45}$$

In order to generalize the results to cases where the dissolution rate can vary with time, the λ term is left inside the integral. The advantage of this formulation is that only λ and $R(t)$ are required to be known, whereas Eq. 42 requires that the moisture content throughout the rice particle be determined.

An even simpler way of calculating the amount of solid removed is motivated by the discrete model for dissolution in Appendix A, where shells of gelatinized solid are removed at particular times. Immediately after, a shell has peeled $R(t) = s(t)$ and the particle contains only the initial uniform moisture content, so that the amount of solid remaining is therefore

$$V_s(t) = \frac{4\pi}{3}(1-\phi_0)R^3(t) \tag{46}$$

Using Eq. 43, the amount of solids dissolved is

$$V_d(t) = \frac{4\pi}{3}(1-\phi_0)\left[1-R^3(t)\right] \tag{47}$$

at exactly the discrete peeling times. Hence, no knowledge of ϕ in the gelatinized layer is required; only information about $R(t)$ is needed. This argument works equally well for the continuous model when the gelatinized thickness $R(t) - s(t)$ is assumed to be small compared to unity. For this case, only a thin gelatinized layer holds moisture above the level ϕ_0 and the approximations above are sufficiently accurate.

Using the approximation (Eq. 47), we now calculate an approximate volume of dissolved solids. If the velocity of $R(t)$ is $v(t)$ then

$$R(t) = 1 - \int_0^t v(\tau)d\tau \tag{48}$$

The velocity is time-dependent if the process temperature varies with time. Using Eq. 48, Eq. 47 can be rewritten as

$$V_d(t) = \frac{4\pi}{3}(1-\phi_0)\left\{1-\left[1-\int_0^t v(\tau)d\tau\right]^3\right\} \tag{49}$$

Clearly, when $\int_0^t v(\tau)d\tau = 1$, dissolution is complete and $V_d(t)$ will remain constant after this time.

Grain with a size distribution

The total dissolved solids for a single rice particle of unit radius is given by Eq. 49. From this, an expression for the total dissolved solids for an arbitrary distribution of grain sizes can be derived.

Consider a sphere of initial (dimensionless) radius η. For times t such that $\int_0^t v(\tau)d\tau \ge \eta$, dissolution is complete and the dissolved solids volume will remain constant. We modify Eq. 49 to give the volume of dissolved solids over time as

$$V_d(\eta,t) = \frac{4\pi}{3}(1-\phi_0) \times \begin{cases} \eta^3 - \left[\eta - \int_0^t v(\tau)d\tau\right]^3 & \text{if } \int_0^t v(\tau)d\tau < \eta \\ \eta^3 & \text{if } \int_0^t v(\tau)d\tau \ge \eta \end{cases} \tag{50}$$

To account for a distribution of particle sizes, we introduce a distribution function $p(x)$. The integral $\int_a^b p(x)dx$ represents the proportion of the number of spheres which have a radius between a and b and summing up all the proportions gives $\int_0^\infty p(x)dx = 1$. Using the scalings we have introduced, the total mass of uncooked rice is $(4\pi/3)\rho l^3 \int_0^\infty x^3 p(x)dx$ where ρ is the average density of uncooked rice. For a discrete distribution of grist of unit radius, we use $p(x) = \delta(1-x)$ where δ is the Dirac delta function.

The total volume of dissolved solids from a distribution of particle sizes as a function of time can then be expressed as

$$V_{td}(t) = \int_0^\infty p(x)V_d(x,t)dx$$

$$= \frac{4\pi(1-\phi_0)}{3}\int_0^{\int_0^t \upsilon(\tau)d\tau} x^3 p(x)dx$$

$$-\frac{4\pi(1-\phi_0)}{3}\int_{\int_0^t \upsilon(\tau)d\tau}^\infty \left[x^3 - \left(x - \int_0^t \upsilon(\tau)d\tau\right)^3\right] p(x)dx \quad (51)$$

The mass fraction of dissolved solids relative to the total mass of solids available may be calculated using the ratio of $V_d(t)$ or $V_{td}(t)$ (where appropriate) to $4\pi(1-\phi_0)/3$. Numerical studies of the cases of uniform grist size and of an arbitrary distribution of grist size are discussed in the following section for various cooking temperature regimes. The two effects (grist size and temperature history) are looked at individually and then in combination.

Numerical solutions for varying temperature and grist sizes

In this section we use results obtained for time-varying temperatures in Appendix B. It will be assumed that changes in $T(t)$ are small enough to approximate D^* in Eq. B5 to unity. Furthermore, we neglect any temperature dependence of ϕ_1 so a natural choice is $\phi_{ref} = \phi_1$ giving $\theta_s = 1$ and $\nu^* = \nu$. Under these conditions, the temperature dependence only appears through $\theta_g(T)$.

A typical simple rule characterizing the gelatinization temperature (in °C) with moisture volume fraction, as illustrated in Figure 1, is

$$T_g = \begin{cases} 70, & \phi_g > 0.7 \\ 175 - 150\phi_g, & \phi_g \le 0.7 \end{cases} \quad (52)$$

In rescaled variables (using Table 1a parameter values), this equation can be rewritten as

$$\theta_g(T) = \frac{1}{90}(145 - T), \quad T \ge 70 \quad (53)$$

When all grist particles are the same size (scaled radius equal to unity), the mass fraction of dissolved solids increases with decreasing peeling thickness (or granule size), as shown in Figure 6. As discussed in the previous sections, the results of the continuous and discrete dissolution models are equivalent on identifying $\lambda = 2\Omega_2/\Delta$. Hence, decreasing Δ is the same as increasing the dissolution rate.

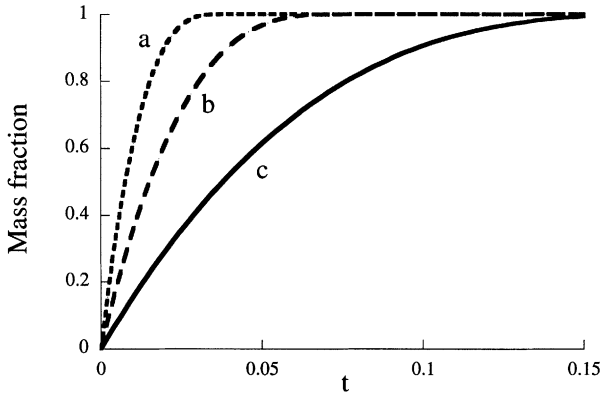

Figure 6. Mass fraction of dissolved starch vs. time at different granule sizes Δ for grist with scaled radius unity: (a) $\Delta = 0.01$ (b) $\Delta = 0.02$ (c) $\Delta = 0.05$.

The parameter values are in Table 1a with $T = 91$°C corresponding to $\theta_g = 0.6$.

The effect of having different, but constant, cooking temperatures is illustrated in Figure 7. When all grist particles are the same size, the mass fraction of dissolved solids increases with cooking temperature. Higher temperatures means that a lower moisture content is required for gelatinization, resulting in a more rapid gelatinization process. For both models, the dissolution speeds increase for higher temperatures.

We next explore the effect of changing the distribution of grist size on the total dissolved solids mass. (Note that the distributions are on a mass basis. To convert to a distribution based on the number of each size, it is necessary to divide by x^3 where x is the radius of the grist in the distribution.) Figure 8 shows the dissolved mass fraction as a function of time when the grist is made up of various proportions of two dif-

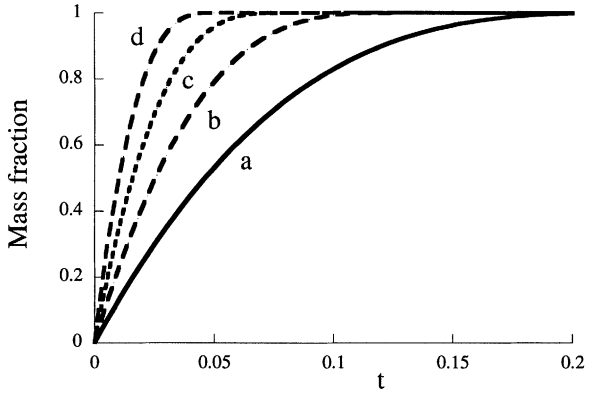

Figure 7. Mass fraction of dissolved starch vs. time at different temperatures (in °C) for grist with scaled radius unity: (a) $T = 70$°C; (b) $T = 80$°C; (c) $T = 90$°C; (d) $T = 100$°C.

The parameter values are in Table 1a with $\Delta = 0.02$.

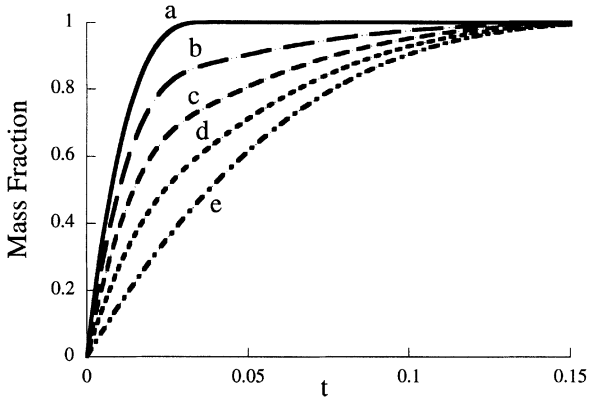

Figure 8. Starch mass fraction dissolved vs. time for various particle mass distributions.

(a) Every particle in the grist with scaled radius 0.5; (b) 3/4 of the mass of grist with scaled radius 0.5 and 1/4 of the mass of grist with scaled radius 2.5; (c) half the mass of grist with scaled radius 0.5 and half the mass of grist with scaled radius 2.5; (d) 1/4 of the mass of grist with scaled radius 0.5 and 3/4 of the mass of grist with scaled radius 2.5; (e) every particle in the grist with scaled radius 2.5. The parameter values are in Table 1a with $\Delta = 0.02$ and $T = 91°C$ corresponding to $\theta_g = 0.6$.

ferent masses. The results show that having smaller grist particles leads to more rapid dissolution. Furthermore, if there is a continuous distribution of grist sizes, Figure 9 shows that a 50/50 mixture of two masses (curve (*b*)) can be accurately approximated for short and long times by continuous distributions which are weighted towards these two masses (curves (*a*) and (*c*), respectively).

Figure 11 shows the dissolution of a normal distribution of particle masses for the three temperature regimes illustrated in Figure 10. The curves show that as the temperature ramping steepens, the dissolved mass fraction increases more rapidly in the early stages. Figure 12 shows the effect of these different temperature regimes, when there are two grist

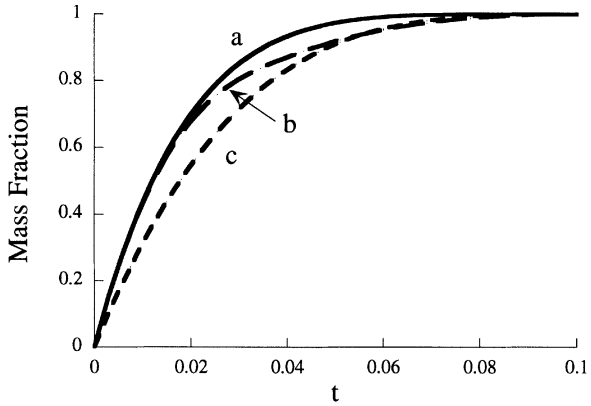

Figure 9. Starch mass fraction dissolved vs. time for various particle mass distributions.

(a) Mass distribution of $(1.5 - x)^2 x^3$, for $0.5 < x < 1.5$; (b) half the mass of grist with scaled radius 0.5 and half the mass of grist with scaled radius 1.5; (c) mass distribution of x^3, between $0.5 < x < 1.5$. The parameter values are in Table 1a with $\Delta = 0.02$ and $T = 91°C$ corresponding to $\theta_g = 0.6$.

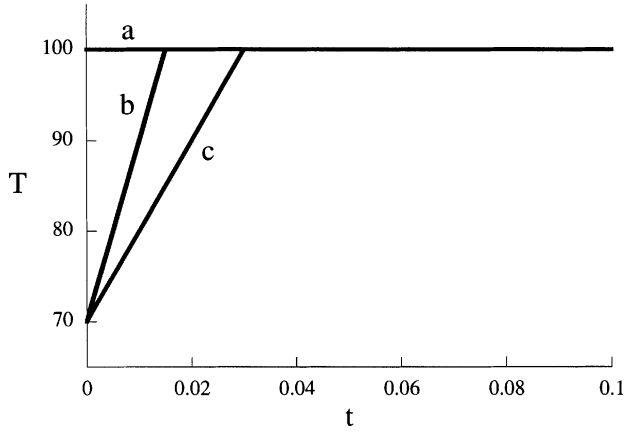

Figure 10. Temperature regime for mass fractions in Figures 11 and 12.

masses. It exhibits the same qualitative behavior as for the normal distribution case in Figure 11.

Condition for dissolution to proceed to completion

It is common knowledge that, if insufficient water is added to rice, then dissolution is not complete. We are interested in estimating the amount of water that needs to be added to the rice grist to achieve full dissolution. This requires that we consider the effect on the dissolution rate λ of an increasing concentration of dissolved solids in the surrounding solution. Hence, we allow the dissolution rate to vary with time. Suppose that λ is proportional to some power of the difference between the liquid concentration in solution and the liquid concentration at the grist outer surface, namely

$$\lambda(t) = k\left(\frac{\phi_{\text{sol}}(t) - \phi_1}{1 - \phi_1}\right)^n \tag{54}$$

where k and n are constants ($n > 0$).

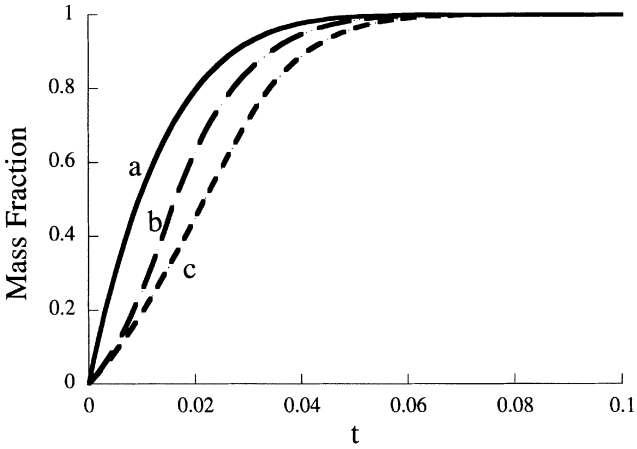

Figure 11. Starch mass fraction dissolved vs. time for a normal mass distribution, mean $x = 1$, namely $e^{-5(x-1)^2}$, for $0.25 < x < 1.75$.

The parameter values are in Table 1a with $\Delta = 0.02$ and Eq. 53. The three curves a, b, c correspond to the three different temperature regimes in Figure 10.

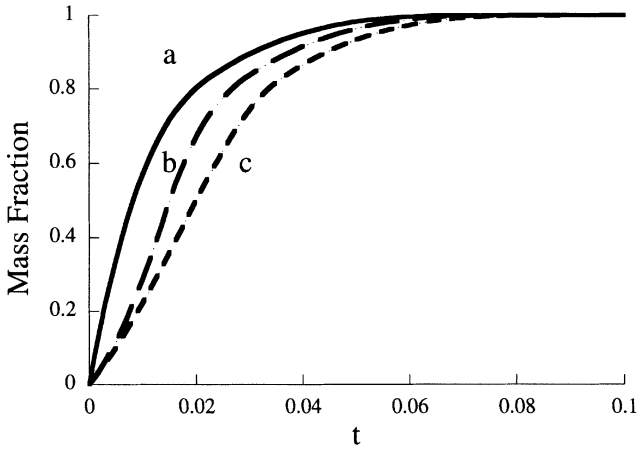

Figure 12. Starch mass fraction mass dissolved vs. time where half the mass of grist with scaled radius 0.5 and the other half with scaled radius 1.5.

The parameter values are in Table 1a with $\Delta = 0.02$ and Eq. 53. The three curves, a, b, c correspond to the three different temperature regimes in Figure 10.

It is now possible that the dissolution rate goes to zero before all of the available starch has dissolved. This will manifest itself as a minimum water-to-rice ratio. Hence, we are seeking the possibility that $\phi_{sol}(t) = \phi_1$ before all of the grist has dissolved.

Let W be the initial volume of water added per unit volume of raw rice and let V_r be the initial volume of the raw rice. To calculate $\phi_{sol}(t)$, we need to take account of the water already in the uncooked raw rice, since this will also be released into solution as the starch dissolves. The total volume of dissolved solids is $V_{td}(t)$; hence, the initial moisture locked inside the raw grist which is also released with the solids is just $\phi_0 V_{td}(t)/(1-\phi_0)$. (We have assumed that all the gelatinized rice is dissolved and, hence, the only water inside the rice is the water that was initially there.) The volume fraction of water in the solution is the ratio of the volume of water to the total volume (dissolved solids plus water)

$$\phi_{sol}(t) = \frac{WV_r + \dfrac{\phi_0}{1-\phi_0} V_{td}(t)}{WV_r + \dfrac{V_{td}(t)}{1-\phi_0}} \tag{55}$$

The dissolution process will be incomplete if $\phi_{sol}(t) = \phi_1$ before all the grist has had time to dissolve. This defines a possible nonmaximum value V_f for dissolved solids volume at the time when dissolution comes to an end. Since $(1-\phi_0)V_r$ is the initial total solids volume available, we can rewrite Eq. 55 as

$$\frac{V_f}{(1-\phi_0)V_r} = \min\left[W\frac{(1-\phi_1)}{(\phi_1-\phi_0)}, 1\right] \tag{56}$$

Consequently, dissolution is incomplete when

$$W < \frac{\phi_1 - \phi_0}{1-\phi_1} \tag{57}$$

(Note that this upper bound is just α defined in Eq. 15.) Hence, for values of W satisfying this constraint, the dissolution does not proceed to completion. Alternatively, if

$$W \geq \frac{\phi_1 - \phi_0}{1-\phi_1} \tag{58}$$

the dissolution process proceeds to completion (assuming that all the starch has the ability to dissolve). Using the values in Table 1a, dissolution completes if $W > 3$.

Common experience suggests this ratio is in the vicinity of 3.5 to achieve reasonable dissolution of rice grist in practice. We can conclude that this fairly simplistic model for surface dissolution is giving ratios of the correct size.

Conclusions

We have presented and solved a model for water uptake and gelatinization, followed by dissolution, for a piece of rice grist. The model has been extended to account for a distribution of particle size, a changing process temperature, and a time-varying dissolution rate.

An analytic solution has been determined using a Fickian diffusion model for water uptake and gelatinization of a swelling spherical rice particle. Typically, for cereal products, the moisture diffusivity is a strongly increasing function of moisture content and the diffusivity is much larger in gelatinized starch than ungelatinized starch. Consequently, as seen experimentally, there is a steep moisture front between the dry/ungelatinized and wet/gelatinized regions of a particle. Gelatinization occurs at a certain moisture concentration, which is dependent on the temperature. It is a reasonable assumption then that gelatinization occurs at the wetting front. In the absence of dissolution, this front moves so that its location is initially proportional to the square root of time, then becomes linear with time, and finally moves at a faster rate as it approaches the center of the rice particle. The time for the entire piece of rice particle to be gelatinized has been calculated as a function of rice characteristics. These factors, which will change with rice variety, include the moisture content at which the starch undergoes the irreversible gelatinization reaction as a function of temperature, the water diffusivity as a function of moisture content, and initial and equilibrium moisture content.

The model also includes the effects of the dissolution or peeling-away of cooked outer parts of the rice particle. Nonzero dissolution leads to a significant increase in the speed of the gelatinization front and linear front speeds during most of the process. This type of linear penetration behavior has been experimentally observed in many complex polymer systems, and has led other researchers (Thomas and Windle, 1982) to significantly modify Fickian models in an attempt to obtain linear behavior. Our work presents a relatively simple extension of Fickian diffusion that is promising in that it exhibits these linear behaviors.

In the case of sufficiently large and constant dissolution rates, both the dissolution and gelatinization fronts move at constant speed and there is a narrow gelatinization region between the fronts. The constant speed of these fronts is proportional to the dissolution rate, and inversely proportional to the thickness of the gelatinized region. The mass of dissolved solids, which initially increases rapidly, begins to level off giving reduced returns at later times. The dissolution process becomes less productive as time proceeds, which has implications for the optimal stopping time in production.

Extending these results to a consideration of the dissolved solids for a distribution of rice particle sizes reveals that smaller particles are dissolved more rapidly and, hence, the amount of dissolved solids initially rises faster than when all particles are the same size. The larger particles in the distribution take longer to dissolve and, hence, there is a more dramatic slowdown in total dissolved solids at later times. Everything in the modeling points to the fact that the dissolution process proceeds faster for small rice grist. However, in production, handling problems may arise when the grist size is too small.

Varying the temperature in the rice cooker influences the speed of the gelatinization and dissolution fronts, and, hence, the amount of total dissolved solids at any given time. If the cost of cooking is calculated as a function of the temperature regime, this model can be used to optimize the temperature regime to lower energy costs. If a certain quantity of total dissolved solids is required, then various temperature regimes will give different processing times. These can be balanced against energy expenditure. The optimization is complicated by the temperature dependence of both the diffusivity and gelatinization moisture content, which will differ with rice variety.

A minimum water-to-rice ratio for complete starch dissolution was determined. Our analysis assumed that all of the available starch could be gelatinized and dissolved. This assumption may not be valid for some rice varieties.

Many factors and parameters influence the cooking process. Only some of these parameters are known for rice (grist size, initial moisture content). The models highlight the combinations of these parameters which are important for determining the rate of starch dissolution. The accurate determination of the diffusivity and its dependence on moisture content, and the gelatinization and equilibrium saturation moisture content as a function of temperature, is still needed for whole grain milled rice before the results in this article can be confidently quantified.

Acknowledgments

This project arose from CUB BrewTech participation at the 1998 Mathematics-in-Industry Study Group, resulting in further collaboration between BrewTech, The University of Melborne, and Victoria University of Wellington. Malcolm Davey wishes to thank CUB BrewTech for its financial support of this project and the knowledge and input brought by Mr. Tony Oliver and Dr. Peter Rogers.

Literature Cited

Bakshi, A. S., and R. P. Sing, "Modelling Rice Parboiling Process," *Lebensm Wiss u Technol*, **15**, 89 (1982).

Bear, J., *Dynamics of Fluids in Porous Media*, Dover, New York (1972).

Biliaderis, C. G., C. M. Page, T. J. Maurice, and B. O. Juliano, "Thermal Characterization of Rice Starches: A Polymeric Approach to Phase Transitions of Granular Starch," *J. Agric. Food Chem.*, **34**, 6 (1986).

de Gennes, P. G., *Scaling Concepts in Polymer Physics*, Corwell University Press, London (1979).

Devotta, I., V. D. Ambeskar, A. B. Mandhare, and R. A. Mashelkar, "The Life Time of a Dissolving Polymeric Particle," *Chem. Eng. Sci.*, **49**, 645 (1994a).

Devotta, I., V. Premnath, M. V. Badiger, P. R. Rajamohanan, and R. A. Mashelkar, "On the Dynamics of Mobilization in Selling-Dissolving Polymeric Systems," *Macromol.*, **27**, 532 (1994b).

Edwards, D. A., and D. S. Cohen, "A Mathematical Model for a Dissolving Polymer," *AIChE J.*, **41**, 2345 (1995).

Fortes, M., M. R. Okos, and J. R. Barrett, "Heat and Mass Transfer Analysis of Intra-Kernel Wheat Drying and Rewetting," *J. Agric. Eng. Res.*, **26**, 109 (1981).

Gomi, Y., M. Fukuoka, T. Mihori, and H. Watanabe, "The Rate of Starch Gelatinization as Observed by PFG-NMR Measurement of Water Diffusivity in Rice Starch/Water Mixtures," *J. Food Eng.*, **36**, 359 (1998).

Herman, M. F., and S. F. Edwards, "A Reptation Model for Polymer Dissolution," *Macromol.*, **23**, 3662 (1998).

Juliano, B. O., "Polysaccharides, Proteins and Lipids," *Rice: Chemistry and Technology*, B. O. Juliano, ed., 2nd ed., American Association of Cereal Chemists, St. Paul, MN, pp. 59–174 (1985).

Juliano, B. O., "Criteria and Tests for Rice Grain Qualities," *Rice: Chemistry and Technology*, B. O. Juliano, ed., 2nd ed., American Association of Cereal Chemists, St. Paul, MN, pp. 443–524 (1985).

Kar, N., R. K. Jain, and P. P. Srivastav, "Parboiling of Dehusked Rice," *J. Food Eng.*, **39**, 17 (1999).

Kirchoff, G., *Vorlesungen uber die Theorie der Warme*, Barth, Leipzig, Germany (1894).

Kunze, W., *Technology Brewing and Malting*, 7th ed. (English Translation), VLB Berlin (1996).

Kustermann, M., R. Scherer, and H. D. Kutzbach, "Thermal Conductivity and Diffusivity of Shelled Corn and Grain," *J. Food Process Eng.*, **4**, 137 (1981).

Landman, K. A., and C. P. Please, "Modelling Moisture Uptake in a Cereal Grain," *IMA J. Math App. in Bus. and Ind.*, **10**, 265 (1999).

Landman, K. A., L. Pel, and E. F. Kaasschieter, "Analytic Modelling of Drying of Porous Materials," *Mathematical Eng. in Industry*, **8**, 89 (2001).

Lund, D. B., and M. Wirakartakusumah, "Engineering and Food," *Proc. of 3rd Int. Congress on Eng. and Food*, B. M. Mckenna, ed., Elsevier Applied Science (1984).

McGowan, P., and M. McGuinness, "Modelling the Cooking Process of a Single Cereal Grain," *Proc. of Mathematics-in-Industry Study Group*, University of South Australia, Adelaide, John Hewitt, ed., 114 (1996).

McGuinness, M., P. Howlett, and Hong Jin, "Process Optimisation of Rice Gelatinisation for Beer Production," *Proc. of Mathematics-in-Industry Study Group*, University of South Australia, Adelaide, J. Hewitt, ed., 132 (1998).

McGuinness, M., C. P. Please, N. Fowkes, P. McGowan, L. Ryder, and D. Forte, "Modelling the Wetting and Cooking of a Single Cereal Grain," *IMA J. Math. App. in Bus. and Ind.*, **11**, 49 (2000).

Papanu, J. S., D. S. Soane, A. T. Bell, and D. W. Hess, "Transport Models for Swelling and Dissolution of Thin Polymer Films," *J. App. Sci.*, **38**, 859 (1989).

Peppas, N. A., J. C. Wu, and E. D. von Meerwall, "Mathematical Modeling and Experimental Characterization of Polymer Dissolution," *Macromolecules*, **27**, 5626 (1994).

Ramesh, M. N., and P. N. Srinivasa Rao, "Development and Performance Evaluation of a Continuous Rice Cooker," *J. Food Eng.*, **27**, 377 (1996).

Ranade, V. V., and R. A. Mashelkar, "Convective Diffusion from a Dissolving Polymeric Particle," *AIChE J.*, **41**, 666 (1995).

Stapley, A. G. F., "Diffusion and Reaction in Wheat Grains," PhD Thesis, University of Cambridge, U.K. (1995).

Stapley, A. G. F., P. J. Fryer, and L. F. Gladden, "Diffusion and Reaction in Whole Wheat Grains During Boiling," *AIChE J.*, **44**, 1777 (1998).

Suzuki, K., K. Kubota, M. Omichi, and H. Hosaka, "Kinetic Studies on Cooking of Rice," *J. Food Sci.*, **41**, 1180 (1976).

Suzuki, K., M. Aki, K. Kubota, and H. Hosaka, "Studies on the Cooking Rate Equations of Rice," *J. Food Sci.*, **42**, 1545 (1977).

Syarief, A. M., R. J. Gustafson, and R. V. Morey, "Moisture Diffusion Coefficients for Yellow-Dent Corn Components," *Forum Pascasarjana*, **9**, 1 (1986).
Takeuchi, S., M. Fukuoka, Y. Gomi, M. Maeda, and H. Watanabe, "An Application of Magnetic Resonance Imaging to a Real Time Measurement of the Change of Moisture Profile in a Rice Grain during Boiling," *J. Food Eng.*, **33**, 181 (1997a).
Takeuchi, S., M. Maeda, Y. Gomi, M. Fukuoka, and H. Watanabe, "The Change of Moisture Distribution in a Rice Grain during Boiling as Observed by NMR Imaging," *J. Food Eng.*, **33**, 281 (1997b).
Tester, R. F., and W. R. Morrison, "Swelling and Gelatinization of Cereal Starches. I. Effects of Amylopectin, Amylose, and Lipids," *Cereal Chemistry*, **67**, 551 (1990).
Thomas, N. L., and A. H. Windle, "A Theory of Case II Diffusion," *Polymer*, **23**, 529 (1982).
Tsiartas, P. C., L. W. Flanagin, C. L. Henderson, W. D. Hinsberg, I. C. Sanchez, R. T. Bonnecaze, and C. G. Willson, "The Mechanism of Phenolic Polymer Dissolution: A New Perspective," *Macromolecules*, **30**, 4656 (1997).
van Beynum, G. M. A., and J. A. Roels, *Starch Conversion Technology*, Marcel Dekker, New York (1985).
Whistler, R. L., J. N. Bemiller, and E. F. Paschall, *Starch: Chemistry and Technology*, 2nd ed., Academic Press, New York (1984).
Zhang, T., A. S. Bakshi, R. J. Gustafson, and D. B. Lund, "Finite Element Analysis of Nonlinear Water Diffusion during Rice Soaking," *J. Food Sci.*, **49**, 246 (1975).

Appendix A: Discrete Interpretation of Dissolution

Consider a rice particle with $R(0)=s(0)=1$, and $\theta(r,0)=0$, for $0 \le r < 1$. Using the gelatinization and water uptake model described in a previous section, water is absorbed into the rice particle and it swells a certain amount. We define a time T_p, when $s(T_p)=1-\Delta$. At this time, the shell of swelled material between R and s is removed from the particle and goes into solution. Hence, at this time, R is reset to $s(T_p)$. Thereafter, the rice particle again swells with water uptake, and the gelatinization model is now solved with new initial conditions $R=s=1-\Delta$. When $s=1-2\Delta$, the next shell peels away. This cycle of gelatinization and removal continues until $s=0$.

Starting with a sphere of unit radius with initial conditions $R(0)=s(0)=1$, we have defined a time T_p, when the first shell is removed, as

$$s_p = s(T_p) = 1-\Delta \tag{A1}$$

The gelatinization model gives a relationship between R and s given by Eq. 25. Hence, the position of the outer boundary at the peeling time can be determined as

$$R_p = R(T_p) = \left[\left(1+\frac{\Omega_1}{\Omega_2}\right) - \frac{\Omega_1}{\Omega_2}(1-\Delta)^3\right]^{1/3} \tag{A2}$$

These values of s_p and R_p allow us to write the peeling time, using Eq. 27, as

$$T_p(\Delta) = \frac{1}{2\Omega_1}\left\{1+\frac{\Omega_1}{\Omega_2} - \left[\left(1+\frac{\Omega_1}{\Omega_2}\right) - \frac{\Omega_1}{\Omega_2}(1-\Delta)^3\right]^{2/3} - \frac{\Omega_1}{\Omega_2}(1-\Delta)^2\right\} \tag{A3}$$

For thin shells ($\Delta \ll 1$), a Taylor series expansion of $T_p(\Delta)$ in terms of Δ gives

$$T_p(\Delta) = \Delta^2\left[\left(\frac{\Omega_1+\Omega_2}{2\Omega_2^2}\right) - O(\Delta)\right] \tag{A4}$$

Since the first term in the series is $O(\Delta^2)$, when Δ is doubled, the T_p increases by a factor of four.

The time of peel off one layer from a dimensionless sphere of unit radius is given by Eq. A3. To generalize this to a sphere of dimensionless radius r $(0<r<1)$, the scaling of length and time are taken into account as given in Eq. 10. The peeling time for a sphere of radius r is r^2 multiplied by the peeling time for a sphere of radius unity. The physical peeling depth $l\Delta$ remains constant. The scaled peeling depth is obtained by dividing the physical peeling depth by the physical radius of the sphere lr, giving the value Δ/r.

The peeling time T_{pr} for a piece of grist of dimensionless radius r is then given in terms of T_p as

$$T_{pr}(r,\Delta) = r^2 T_p\left(\frac{\Delta}{r}\right) \tag{A5}$$

Note that

$$T_{pr}(1,\Delta) = T_p(\Delta) \tag{A6}$$

Using the expansion (Eq. A4), we find that

$$T_{pr}(r,\Delta) = r^2 T_p\left(\frac{\Delta}{r}\right) = \Delta^2\left[\left(\frac{\Omega_1+\Omega_2}{2\Omega_2^2}\right) - \frac{1}{r}O(\Delta)\right] \tag{A7}$$

This shows that the radius of the sphere does not affect the peeling time when $r \gg \Delta$. Comparing Eqs. A4 and A7, we observe that if $r<1$ then $T_{pr} < T_p$, and

$$T_{pr}(r,\Delta) = T_p(\Delta)\left[1-\left(\frac{1}{r}-1\right)O(\Delta)\right] \tag{A8}$$

Therefore, if $\Delta \ll r$ we have

$$T_{pr}(r,\Delta) \approx T_p(\Delta) \tag{A9}$$

Evaluating T_{pr} as a function of r, as plotted in Figure A1, shows that this approximation is in fact valid for a large range of r values.

The total time for dissolution T_d can now be determined by summing up the peeling times for each layer as $s \to 0$ in steps of Δ. Since the physical size of a rice particle is l, and the physical size of a layer is $l\Delta$, the number of layers to be peeled off is $1/\Delta$. Without much loss of accuracy for small Δ, we assume that $1/\Delta$ is an integer. The nondimensional radius after each layer is peeled off will be a multiple of Δ, that is, $r=i\Delta$ where $i=1,2,\ldots,1/\Delta$. The total dissolution time T_d is then given by the sum

$$T_d = \sum_{i=1}^{1/\Delta} T_{pr}(i\Delta,\Delta) \tag{A10}$$

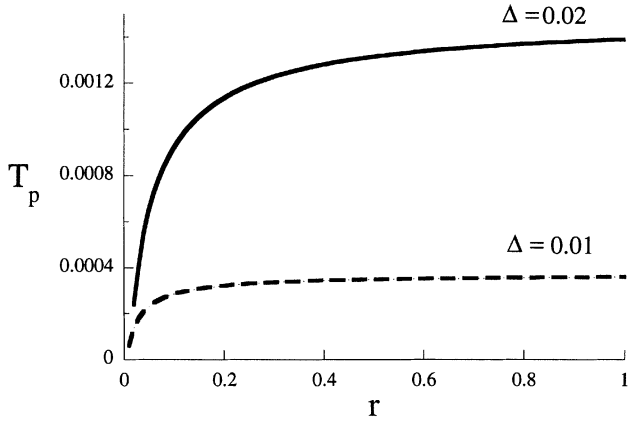

Figure A1. $T_{pr}(r,\Delta)$ vs. r $(\Delta < r < 1)$ using parameter values in Table 1a, $\theta_g = 0.6$ and $\Delta = 0.01$ and 0.02.

This expression may be approximated by a simpler expression using Eq. A9. An approximate dissolution time (which is also an upper bound on the actual dissolution time) is given by

$$T_d \approx \frac{T_p(\Delta)}{\Delta} \tag{A11}$$

To demonstrate this graphically, in the limit as $\Delta \to 0$, the sum in Eq. A10 can be replaced by an integral, giving

$$T_d \approx \frac{1}{\Delta}\int_{\Delta}^{1} T_{pr}(r,\Delta)\,dr$$

Since this integral represents the area under the curve in Figure A1 and the curve is well approximated by a constant when Δ is sufficiently small, the approximation (Eq. A11) follows.

The time T_d can be further simplified using the expansion (Eq. A4), giving

$$T_d \approx \left(\frac{\Omega_1 + \Omega_2}{2\Omega_2^2}\right)\Delta + O\left[\Delta^2 \ln(\Delta)\right] \tag{A12}$$

Consequently, for thin shell layers, the dissolution time is proportional to the shell thickness Δ, that is, the dissolution time is linear in Δ.

An approximate velocity for the gelatinization front can be calculated for this model. For a sphere of radius r, the front travels a distance Δ from the surface in the peeling time $T_{pr}(r,\Delta)$. This gives an estimate of the average velocity for each step as

$$\frac{\Delta}{T_{pr}(r,\Delta)} \tag{A13}$$

Alternatively, over the entire dissolution process for a sphere with a dimensionless radius of unity, the average velocity is $1/T_d$. Using the approximation for T_d from Eq. A11, this velocity is

$$v_{av} = \frac{1}{T_d} \approx \frac{\Delta}{T_p(\Delta)} \approx \left(\frac{2\Omega_2^2}{\Omega_1 + \Omega_2}\right)\frac{1}{\Delta} \tag{A14}$$

Consistent with our previous arguments, the average velocity over the whole process is well approximated by the average velocity of the first peeling step.

To calculate an approximate equivalent dissolution rate for the discrete model, the amount of swelling is determined. From Eq. A2, for $\Delta \ll 1$, we obtain

$$R_p = 1 + \frac{\Omega_1}{\Omega_2}\Delta + O(\Delta^2) \tag{A15}$$

Therefore, as s reduces by Δ, R increases by $(\Omega_1/\Omega_2)\Delta$ (correct to first order in Δ). This implies that the thickness removed after swelling is

$$R_p - s_p = \Delta\left(1 + \frac{\Omega_1}{\Omega_2}\right) + O(\Delta^2) \tag{A16}$$

Therefore, before each layer is removed, $[1 + (\Omega_1/\Omega_2)]$ is the factor by which each layer swells.

To calculate an average rate of removal, we divide $R_p - s_p$ by $T_p(\Delta)$ using its asymptotic expansion (Eq. A4), and obtain

$$\frac{R_p - s_p}{T_p} = \frac{2\Omega_2}{\Delta} + O(1) \tag{A17}$$

Then, the continuous and the discrete dissolution models give the same rate of dissolution if, to leading order

$$\frac{2\Omega_2}{\Delta} = \lambda = \frac{\Omega_1 + \Omega_2}{\delta_p} \tag{A18}$$

This equation serves to relate the continuous and the discrete models, and (since $l\Delta$ is a physical starch granule size) it may be regarded as providing a physical meaning for the continuous dissolution rate λ.

Note that the same result is obtained if the average speed of dissolution of the discrete model, given by Eq. A14, is equated to the speed of dissolution of the continuous model, given by Eq. 35. Notice that the ratio of the dissolution rate and the dissolution front speed, that is, λ/v_d equals $[1 + (\Omega_1/\Omega_2)]$; this factor accounts for the swelling of the spherical particle. For the dissolution front and the gelatinization front to move at the same rate, the dissolution rate has to be larger than the speed of the gelatinization front to counter the effect of swelling. Equation A18 implies that the layer thickness in the continuous and discrete models are related as

$$\delta_p = \left(1 + \frac{\Omega_1}{\Omega_2}\right)\frac{\Delta}{2} \tag{A19}$$

This relationship may be usefully interpreted geometrically with the help of Figure A2. During one peeling event, the outer grain radius R_d and the gelatinization front s_d for the discrete model are represented by the heavy curves. The straight line joining A to B represents the gelatinization front traveling at the average gelatinization velocity for the discrete model. This is required to match the actual gelatiniza-

tion front position for the continuous model, which we call $s(t)$. Because of the $\sqrt{t}$ behavior of s_d, the slope of the line joining AB matches the slope of the curve s_d at point C located a distance $\Delta/2$ below the point A. Hence, the vertical distance CD represents the half-granule thickness $\Delta/2$ multiplied by the swelling factor $[1+(\Omega_1/\Omega_2)]$. We identify this with the length δ_p. This is the (fixed) gelatinization thickness for the continuous model. Therefore, for the continuous model, the outer radius $R(t)$ is obtained by translating the line $s(t)$ vertically upwards by the distance δ_p, as seen in Figure A2 (the distance AE = BF = δ_p).

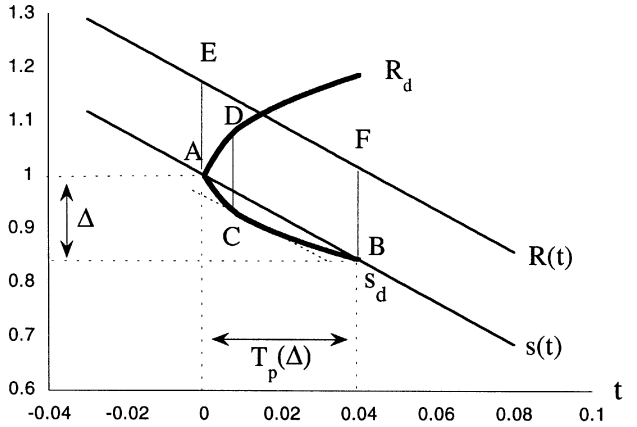

Figure A2. Equivalence of the discrete and continuous dissolution models.

Appendix B: Varying Temperature for a Single Grain

It is usual for the temperature of the rice cooker to vary over the time span of the process, hence, $T = T(t)$. In this Appendix we investigate the effect this varying temperature has on our models. The temperature can affect the process in three ways, namely, through the functional dependence of the diffusivity $D(\phi,T)$ and through the gelatinization and saturation equilibrium moisture contents $\phi_g(T)$ and $\phi_1(T)$, respectively.

Allowing for a temperature dependence in the saturation equilibrium moisture volume fraction means that we can no longer scale the variables with $\phi_1(T)$ and transform the partial differential equations to the same simple type. We introduce a fixed reference moisture volume fraction ϕ_{ref} and now scale all variables with respect to this as

$$\theta = \frac{\phi - \phi_0}{\phi_{\text{ref}} - \phi_0}, \quad \bar{t} = \frac{D(\phi_{\text{ref}}, T(0))}{l^2} t,$$

$$\mathfrak{D}(\theta,T) = \frac{D(\phi,T)}{D[\phi_{\text{ref}},T(0)]} \quad \text{(B1)}$$

The dimensionless equation again takes the form of a nonlinear diffusion problem (Eq. 11), but now the boundary conditions are in terms of two new functions as

$$\theta(R(t),t) = \frac{\phi_1(T) - \phi_0}{\phi_{\text{ref}} - \phi_0} \equiv \theta_s(T),$$

$$\theta(s(t),t) = \frac{\phi_g(T) - \phi_0}{\phi_{\text{ref}} - \phi_0} \equiv \theta_g(T) \quad \text{(B2)}$$

Assuming again that the diffusivity increases exponentially with concentration and taking the usual Arrhenius dependence on temperature, the diffusivity as a function of temperature and moisture content can be expressed as (McGuinness et al., 1998; Stapley, 1995)

$$D(\phi,T) = Ae^{-\mathcal{E}_a/(RT)}e^{c\phi} \quad \text{(B3)}$$

where R is the universal gas constant and $\mathcal{E}_a$ is an activation energy. The modified scaled diffusivity function has the form

$$\mathfrak{D}(\theta,T) = D^*(T)e^{\nu^*(\theta-1)} \quad \text{(B4)}$$

where we define

$$D^*(T) = e^{-(\mathcal{E}_a/R)(1/T - 1/T(0))}, \quad \nu^* = c(\phi_{\text{ref}} - \phi_0) \quad \text{(B5)}$$

The integrated diffusivity function Γ now varies with temperature as well and becomes

$$\Gamma(\theta,T) = \frac{D^*(T)}{\nu^*}(e^{\nu^*(\theta-1)} - e^{-\nu^*}) \quad \text{(B6)}$$

Note that for a time-dependent temperature $T(t)$, the functions $D^*(T)$ and $\Gamma(\theta,T)$ are also implicitly functions of time.

Various equations and parameters from previous sections must be modified to account for a time-dependent temperature. Equations 21–22 determining the time evolution of R and s for gelatinization remain valid, but now the parameters Ω_1 and Ω_2 will vary with temperature, as

$$\Omega_1(T) = \alpha\left[\Gamma(\theta_s,T) - \Gamma\left(\theta_g(T),T\right)\right] \quad \text{(B7)}$$

$$\Omega_2(T) = \frac{\Gamma(\theta_s,T) - \Gamma\left(\theta_g(T),T\right)}{\theta_g(T)} \quad \text{(B8)}$$

The instantaneous dissolution velocity v_d becomes

$$v_d = \frac{\Omega_2}{\delta_p} = \frac{\lambda\Omega_2}{\Omega_1 + \Omega_2} = \frac{\lambda}{\alpha\theta_g(T) + 1} \quad \text{(B9)}$$

In terms of the equivalent discrete dissolution interpretation, the average velocity of the dissolution front v_{av} is modified to become

$$v_{av} = \frac{2\Omega_2^2}{\Omega_1 + \Omega_2}\frac{1}{\Delta} = \frac{2\left[\Gamma(\theta_s,T) - \Gamma\left(\theta_g(T),T\right)\right]}{\theta_g(T)\left(\alpha\theta_g(T) + 1\right)}\frac{1}{\Delta} \quad \text{(B10)}$$

These velocities may be matched by an appropriate identification of parameters (see Eq. A18).

Finally, an approximation for the distance traveled by the dissolution front in time t can be calculated using the expression

$$\int_0^t v(T(\tau))d\tau \quad \text{(B11)}$$

where v is identified with either v_d or v_{av}.

Manuscript received Dec. 19, 2000, and revision received Feb. 4, 2002.